


Influence of dynamic core-electron polarization on the structural minimum in high-order harmonics of CO₂ molecules

Cam-Tu Le * and Dinh-Duy Vu

Atomic Molecular and Optical Physics Research Group, Advanced Institute of Materials Science, Ton Duc Thang University, Ho Chi Minh City, Vietnam
and *Faculty of Applied Sciences, Ton Duc Thang University, Ho Chi Minh City, Vietnam*

Cong Ngo

Ho Chi Minh City Institute of Physics, Vietnam Academy of Science and Technology, 1 Mac Dinh Chi Street, District 1, Ho Chi Minh City, Vietnam

Van-Hoang Le †

Department of Physics, Ho Chi Minh City University of Education, 280 An Duong Vuong Street, District 5, Ho Chi Minh City, Vietnam



(Received 7 September 2019; revised manuscript received 19 October 2019; published 25 November 2019)

The laser-induced dynamic core-electron polarization (DCEP) was known critical in the ionization of polar molecules such as CO, but less relevant in that of nonpolar ones, such as CO₂, N₂, or O₂. For the harmonic process, the DCEP is proven to play an essential role for the polar molecule CO; it affects the harmonic intensity through the ionization at a specific instant. However, the influence of DCEP on the harmonic process of nonpolar molecules is still questionable. In this paper, we show that DCEP can affect the high-order harmonic generation (HHG) through a different mechanism—suppressing the distortion of the laser field on the highest occupied molecular orbital (HOMO) during the recombination phase, thus partially recovering the HOMO symmetry. Consequently, this shifts and sharpens the minima in the HHG spectra, which arise from the two-center interference. To support our point, we provide reliable numerical simulation by solving the time-dependent Schrödinger equation of the coupled CO₂ molecule-laser field within the single active electron framework. From the minima location, we also extract the internuclear separation O–O of CO₂, which is more accurate if including the DCEP in the simulation.

DOI: [10.1103/PhysRevA.100.053418](https://doi.org/10.1103/PhysRevA.100.053418)

I. INTRODUCTION

High-order harmonic generation (HHG) [1,2] from atoms and molecules has been studied for more than three decades and formed the foundation of attosecond physics [3–7]. The HHG spectra of monoatomic gases contain only odd orders harmonics. For multiatomic gases with the more complex potential landscape, the HHG spectra exhibit richer features. The most prominent one is the interference effect arising from the geometry of the molecule [8–16]. It is noted that the interference effect can also be seen in the laser-induced electron diffraction spectra [17–19]. In HHG spectra, the interference between the radiation emitted from different atoms in the molecule manifests as minima whose positions depend on the molecular alignment. For this reason, these minima are also called structural minima.

To explain or predict these minima positions, the authors [8,9] proposed the two-center model based on the recombination matrix element. In spite of the simple formula, the two-center interference model can predict many experimental

observations [15,20–28]. Moreover, even though the two-center model was first applied to symmetric molecules, it can also be extended to asymmetric ones such as CO [29–31], N₂O [28,32], or OCS [28,33]. However, this model cannot describe the experimental feature of the harmonic spectrum from simple molecules such as N₂. Despite the theoretical prediction [34,35], the two-center interference minima have not been observed in some experiments [25,26,36–38]. The reasons may originate from the structure of the highest occupied molecular orbital (HOMO) [39] and the distorted orbital by the laser field, which is shortly called laser-deformed orbitals [40].

The structural minima in the HHG spectra contain some important information and can be used to study the bond symmetry [9], extract the internuclear separation [22,32], probe the attosecond nuclear motion [14], or determine the sign of transition dipole moment [3]. From early works, it has been assumed that the HHG spectra reflect the geometry of the HOMO [3,20,21,23]. However, depending on targets and laser parameters, the role of multiple orbitals in the HHG process has been shown for N₂ and CO₂ [41–43]. The destructive interference between different orbitals gives rise to the dynamical minima [15,42,44], whose positions strongly depend on the laser intensity. If focusing on the structural

*lethicamtu@tdtu.edu.vn

†hoanglv@hcmue.edu.vn

minima originated from the HOMO, one should choose the laser parameter such that the contribution from inner-valence orbitals can be ignored [43]. In this regime, one can use the single active electron (SAE) approximation when solving the time-dependent Schrödinger equation (TDSE), which is denoted the TDSE + SAE method, to simulate the HHG of molecules.

The multielectron residue effects can be mapped into an effective dynamic core-electron polarization (DCEP). We note that the effect of DCEP on the ionization and harmonic processes has been shown important for atoms and molecules [45–51]. For polar molecules CO, the role of DCEP is critical to match the results of single active orbital and SAE with the experiment [47], and with full calculation [49–51], whereas the influence of DCEP on the total ionization probability when the laser is turned off is insignificant for nonpolar molecules such as CO₂, N₂, O₂, and even for polar molecules NO [50]. However, our previous work [51] pointed out that the DCEP affects the harmonic intensity through the ionization around a specific moment, not through the total ionization. Therefore, the effect of the DCEP on the harmonic spectra from nonpolar molecules is necessary to study. Furthermore, we expect that the DCEP can also influence the structural minima through channels other than the ionization process. To clarify this point is the goal of our paper.

This work aims to study the two-center interference as well as to examine the effect of DCEP on the harmonic process of nonpolar molecules, particularly on the structural minima. We choose CO₂ molecule because it is one of the most popular candidates for HHG experiments [15,20–28,42,52] and its spectra display a pronounced minimum. Besides, CO₂ has small polarizability; thus we can check the correlation between the field distortion on orbital and the harmonic process. First, we demonstrate the reliability of generating the HHG spectra from CO₂ molecules by the TDSE + SAE method. Then we study the influence of DCEP on the harmonic intensity as well as the structural minima via the orbital distortion. Finally, using the structural minima in the HHG spectra, we retrieve the internuclear separation of the CO₂ molecule and assess the effect of DCEP on the retrieval.

The rest of the paper has the following structure. In Sec. II, we briefly describe the calculation method. Section III presents the results and discussion about the influence of DCEP on the HHG intensity and the retrieval of the internuclear distance. The final section will conclude this paper. The atomic units are used throughout this paper unless stated otherwise.

II. THEORETICAL MODEL

In the length gauge and dipole approximation, the 3D single-electron time-dependent Schrödinger equation describing the interaction between the active electron of a linear molecule and a laser electric field $\mathbf{E}(t)$ reads as

$$i \frac{\partial}{\partial t} \Psi(\mathbf{r}, t) = \left[-\frac{\nabla^2}{2} + V_{\text{SAE}}(\mathbf{r}) + \mathbf{E}(t) \cdot \mathbf{r} + V_{\text{P}}(\mathbf{r}, t) \right] \Psi(\mathbf{r}, t), \quad (1)$$

where $V_{\text{SAE}}(\mathbf{r})$ is the single active electron potential constructed as in Ref. [53] with the initial wave functions

obtained from GAUSSIAN package [54]. The SAE potential for CO₂ is constructed with the parameters taken from LB94 model [55] as $\alpha = 1.0$ and $\beta = 0.05$. The third term in Eq. (1) is the interaction potential between the active electron and the laser electric field. The influence of the dynamic core-electron polarization is modeled by the polarization potential $V_{\text{P}}(\mathbf{r}, t)$ given in Refs. [45,47] as

$$V_{\text{P}}(\mathbf{r}, t) = -\frac{\hat{\alpha}_c \mathbf{E}(t) \cdot \mathbf{r}}{r^3}. \quad (2)$$

To remove the singularity when r approaches zero, we also apply the cutoff for V_{P} , i.e., at $r \leq r_c$, the polarization potential cancels the laser electric field [45,47]. $\hat{\alpha}_c$ in Eq. (2) is the total polarizability tensor of core electrons whose element values are derived by fitting the energy of the system interacting with a weak field to the Stark effect formula [50]. We assume that the CO₂ molecule is perfectly aligned along the alignment pulse denoted as the z axis and the nuclei are fixed at the equilibrium value $R_{\text{O-O}} = 4.41$ a.u. Therefore, the nonzero components of the tensor are only $\alpha_{xx} = 9.95$, $\alpha_{yy} = 24.06$ [50]. The frozen nuclei assumption is valid based on the fact that the nuclei are much heavier than the electron. Thus it is reasonable to ignore the nuclear motion within the short time frame of the 8 fs laser pulse used in this paper.

The time-dependent wave function $\Psi(\mathbf{r}, t)$ is expanded as a linear combination of the eigenfunctions of the time-independent Schrödinger equation (TISE)

$$\Psi(\mathbf{r}, t) = \sum_{m=-\infty}^{\infty} \sum_{n=1}^{\infty} C_n^m(t) \Phi_n^m(\mathbf{r}), \quad (3)$$

where $\Phi_n^m(\mathbf{r})$ are obtained by using B -spline functions [56] and spherical harmonics. The time-dependent coefficients $C_n^m(t)$ are solved numerically by the fourth-order Runge-Kutta method as our previous work [51]. The computational parameters are chosen carefully to obtain the convergence.

After obtaining the time-dependent wave function, one can calculate harmonics polarized along direction \hat{e} through the Fourier transform of the acceleration dipole $\mathbf{a}(t)$ as

$$S_{\hat{e}}(\omega) \propto |\hat{e} \cdot \mathbf{a}(\omega)|^2, \quad (4)$$

or the dipole moment $\mathbf{d}(t)$ as

$$S_{\hat{e}}(\omega) \propto |\hat{e} \cdot \mathbf{d}(\omega)|^2. \quad (5)$$

Here, ω is the harmonic frequency; $\mathbf{a}(\omega) = \int \mathbf{a}(t) e^{-i\omega t} dt$ and $\mathbf{d}(\omega) = \int \mathbf{d}(t) e^{-i\omega t} dt$ are the Fourier transform of the acceleration dipole and dipole moment, respectively. The harmonic intensity can also be read from $\mathbf{v}(\omega)$, where $\mathbf{v}(\omega)$ is the Fourier transformed velocity dipole in the velocity form [57,58]. With the help of Ehrenfest theorem, we have the relations

$$\mathbf{a}(t) = \frac{d^2}{dt^2} \mathbf{d}(t), \quad (6)$$

$$\mathbf{v}(t) = \frac{d}{dt} \mathbf{d}(t). \quad (7)$$

In this paper, we use Eqs. (4) and (6) to obtain the HHG spectra. In principle, physical results should not depend on gauges and forms provided that the wave functions are exact. However, as figured out by the work [59], based on the accurate numerical solutions of hydrogen atom, if utilizing few-cycle

or very strong pulses ($\sim 10^{15}$ W/cm²), the harmonic spectra from the dipole moment are not reliable. Moreover, one can also use the acceleration dipole but calculated from the molecular potential V , i.e., $\mathbf{a}(t) = -\langle \Psi(t) | \nabla V + \mathbf{E}(t) | \Psi(t) \rangle$ [11,60]. On the one hand, this form is sensitive to the wave function near the nuclei [46,60], hence requiring a denser spatial grid to get the more accurate wave function. The acceleration form in Eq. (6), on the other hand, primarily needs the wave function at large distances, where the effect of the molecular potential becomes weak. In this work, because we utilize a few-cycle laser pulse and the multielectron effect is only described asymptotically through the SAE approximation, the acceleration form calculated from the dipole moment is preferable. The HHG spectra of CO₂ molecules are calculated and analyzed with polarization \hat{e} parallel to the laser polarization. We note that, for the laser parameters used in our study, the HHG spectra from the acceleration and velocity forms are approximately the same.

III. INFLUENCE OF DYNAMIC CORE-ELECTRON POLARIZATION ON THE STRUCTURAL MINIMUM IN HIGH HARMONIC SPECTRA OF CO₂ MOLECULES

A. Structural minimum in high harmonic spectra of the CO₂ molecule

In this work, we use a linearly polarized probe laser whose field lies in the yz plane and is given as

$$E(t) = E_{\max} \sin^2\left(\frac{\pi t}{\tau}\right) \sin(\omega_0 t + \phi_{\text{CEP}}), \quad (8)$$

in which E_{\max} , τ , ω_0 and ϕ_{CEP} are the amplitude peak, duration, frequency, and carrier envelope phase (CEP) of the laser field, respectively. To investigate the influence of DCEP, we utilize the laser of three optical cycles ($\tau \approx 8$ fs). For such a few-cycle laser, the CEP is important in the laser-matter interaction [59,61–64]. In this work, we use two CEPs equal to π and $3\pi/2$, for which the classical calculations have shown that the ionization and recombination in the second cycle are most essential to the HHG spectra. The other parameters are the wavelength of 800 nm ($\omega_0 = 0.057$ a.u.) and the maximum electric field strength of $E_{\max} = 0.0755$ a.u. corresponding to the laser intensity of $I_0 = 2 \times 10^{14}$ W/cm². The HHG spectra are calculated for different angles between the molecular axis and the laser field, $\theta = 0^\circ$ – 90° with step $\Delta\theta = 5^\circ$.

First, we study the ionization probability

$$P_i(t) = 1 - \sum_{\substack{n, m \\ E_n^m < 0}} |\langle \Phi_n^m(\mathbf{r}) | \Psi(\mathbf{r}, t) \rangle|^2, \quad (9)$$

where E_n^m is the eigenvalue corresponding to the eigenfunction Φ_n^m . The results confirm that the inclusion of DCEP does not affect the total ionization of CO₂ when the laser is turned off at $t = \tau$ [50]. Moreover, in contrast to CO molecules [51], the modulation of the ionization probability of CO₂ is insensitive to the two values of CEP, as shown in Fig. 1.

For the harmonics process, based on our previous work [51], one can predict the effect of DCEP on the harmonic intensity by looking at the ionization rate at the time t_1 at which, if ionized, the electron can recombine to the parent

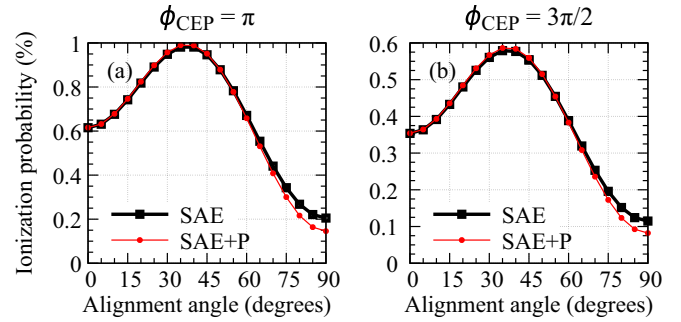


FIG. 1. Ionization probability as a function of alignment angles of the CO₂ molecule illuminated by a three-cycle 800 nm laser with $E_{\max} = 0.0755$ a.u. at $t = \tau$ for two CEPs: (a) $\phi_{\text{CEP}} = \pi$ and (b) $\phi_{\text{CEP}} = 3\pi/2$. The calculations are performed within the SAE approximation with and without the DCEP denoted by SAE + P (red lines with dots) and SAE (black lines with squares), respectively.

ion and emit a photon with the frequency corresponding to the cutoff. The ionization rate is calculated as the formula in Ref. [65]

$$\Gamma(t) = -\frac{d[\ln P_b(t)]}{dt}, \quad (10)$$

where $P_b(t)$ is the survival probability. In practice, because the projection of the solution of TDSE onto the bound states can depend on the gauge that describes the laser-matter interaction, the time-dependent ionization rate can also be gauge dependent. Within the strong-field approximation, the molecular ionization in the length and velocity gauges were performed for N₂ molecules [66]. The results show an agreement between the experimental data and the length gauge result. To the best of our knowledge, there are few works in which the time-dependent ionization rate is obtained from *ab initio* methods such as TDSE (see, for example, Refs. [65,67]), where the length gauge is used and there is no discussion on the gauge dependence. Recently, another approach to obtain the ionization rate that is gauge independent is given in the work [68].

As shown in Fig. 2, the insignificant change of the ionization rate when including the DCEP suggests the minor role of DCEP on harmonic intensities. However, as can be seen from Fig. 3, this prediction is true only for $\theta \geq 60^\circ$. Remarkably, for $\theta = 0^\circ$ – 45° and at orders around the minima, HHG intensities calculated by the two methods, i.e., SAE and SAE + P, differ from one to two orders of magnitude.

The high-order harmonic spectra of CO₂ have the following typical feature: the cutoff order is about 35th for $\phi_{\text{CEP}} = \pi$ and about 37th for $\phi_{\text{CEP}} = 3\pi/2$. These cutoff orders obey the formula obtained from the Lewenstein model with the quantum correction $\omega_{\text{cutoff}} = 1.32I_p + E_{\text{kin}}$ [69], where I_p is the ionization potential and E_{kin} is the maximum kinetic energy acquired by the free electron from the laser field. Particularly, for $\phi_{\text{CEP}} = \pi$, $E_{\text{kin}} \approx 2.89U_p$; and for $\phi_{\text{CEP}} = 3\pi/2$, $E_{\text{kin}} \approx 3.17U_p$ [51], where $U_p = E_{\max}^2/(4\omega_0^2)$ is the ponderomotive energy. Between SAE and SAE + P simulations, the latter has deeper minima located at higher frequency than the former; see Fig. 3(a), Fig. 3(e), and Fig. 5. Especially for $\theta = 45^\circ$, the minimum predicted by the two-center interference model is

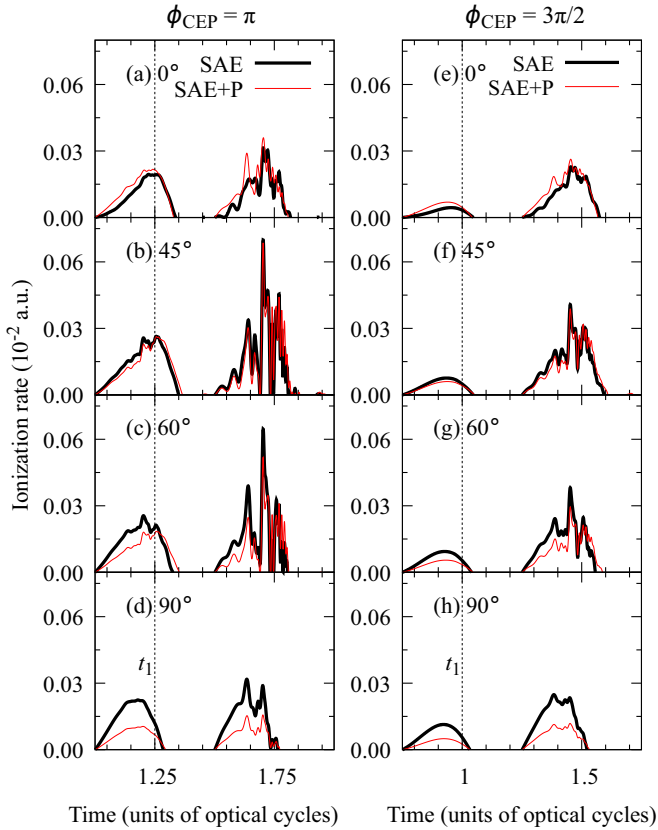


FIG. 2. Same as Fig. 1 but for the ionization rates of the CO_2 molecule with and without DCEP, i.e., SAE + P (thin red lines) and SAE (thick black lines), for different alignment angles from 0° to 90° in two cases of CEP: left panels (a)–(d) for $\phi_{\text{CEP}} = \pi$ and right panels (e)–(h) for $\phi_{\text{CEP}} = 3\pi/2$. The vertical dash lines mark the time t_1 : left panels (a)–(d) with $t_1 = 1.25T$ and right panels (e)–(h) with $t_1 = T$.

about 36th order, very close to the cutoff. This circumstance leads to the cutoff recession [27,70] that can be seen clearly for both $\phi_{\text{CEP}} = \pi$ and $\phi_{\text{CEP}} = 3\pi/2$ in Figs. 3(b) and 3(f), respectively. For $\theta > 45^\circ$, the structural minima are located at higher orders beyond the cutoff of the HHG spectra.

The deeper and slightly higher energy of the structural minima of CO_2 can be explained by the laser-deformed orbital; see Fig. 4. In this figure, we illustrate the orbitals π_g for $\theta = 0^\circ$ and 60° in the case of $\phi_{\text{CEP}} = \pi$ when $|\mathbf{E}| = E_{\text{max}}$ within SAE and SAE + P calculations. One can see that the HOMO without DCEP is distorted by the laser field into an asymmetric dumbbell. To qualitatively understand the relation between HOMO distortion and HHG structural minima, we model the interference by two unbalanced point emitters by

$$A(k, \theta) \propto A_1 - A_2 \exp\{ikR \cos \theta\}, \quad (11)$$

where the minus sign is due to antisymmetry of the molecular orbital and k is the wave number of a returning electron. A_1, A_2 are amplitudes of HHG emitted when the continuum electron recombines with the atomic orbital of the first and second O atoms, respectively. Without the external laser field, the CO_2 molecule has inversion symmetry; thus A_1 and A_2 are identical. In the presence of the laser field, the symmetry is broken, making A_1 different from A_2 . In reality, due to the small

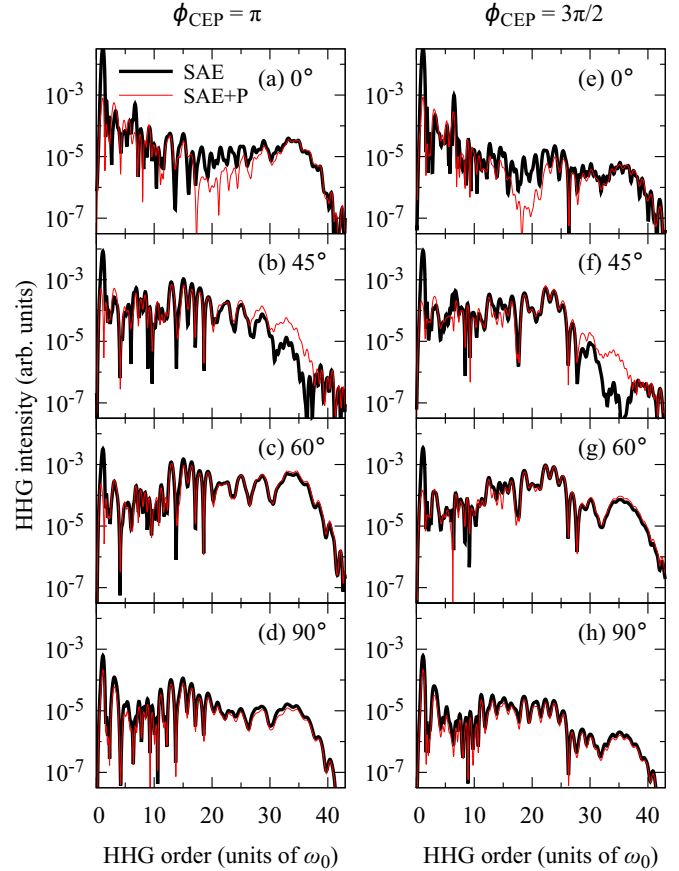


FIG. 3. High-order harmonic spectra in SAE (black thick lines) and SAE + P (thin red lines) of the CO_2 molecule interacting with a laser of three cycles, 800 nm, $E_{\text{max}} = 0.0755$ a.u. in two cases of CEP: left panels (a)–(d) for $\phi_{\text{CEP}} = \pi$ and right panels (e)–(h) for $\phi_{\text{CEP}} = 3\pi/2$. The core electron effect is important in the region around the structural minima.

polarizability of CO_2 , the laser-deformed orbital can be ignored while calculating the HHG spectra [71]. Indeed, except for the destructive minima, a small difference between A_1 and A_2 should not have any observable consequences. However, the minimum location at $kR \cos \theta = 2n\pi + \text{Arg}(A_2/A_1)$ with n as a non-negative integer and their intensity $(|A_1| - |A_2|)^2$ are very sensitive to this small unbalance because of the external laser field. Core polarization, if included, generates an extra field in the opposite direction, thus counteracting the effect of the laser field. As a result, the HOMO calculated with DCEP exhibits a higher degree of symmetry and is closer to the free molecule case; see Figs. 4(c) and 4(d). As in Eq. (11), this brings A_2 closer to A_1 , thus simultaneously shifting and deepening the structural minima as can be seen in Fig. 5. We emphasize that the vertical shift in the log scale represents the ratio between the DCEP correction and the HHG intensity within the SAE model. Due to the small magnitude of orbital deformation, the DCEP correction is also much smaller than the typical intensity of HHG spectra. Thus the shift due to DCEP is only visible when the HHG intensity is sufficiently low, i.e., around the minima or after the cutoff. Away from these positions, the correction is much smaller than the uncorrected HHG intensity, making the shift

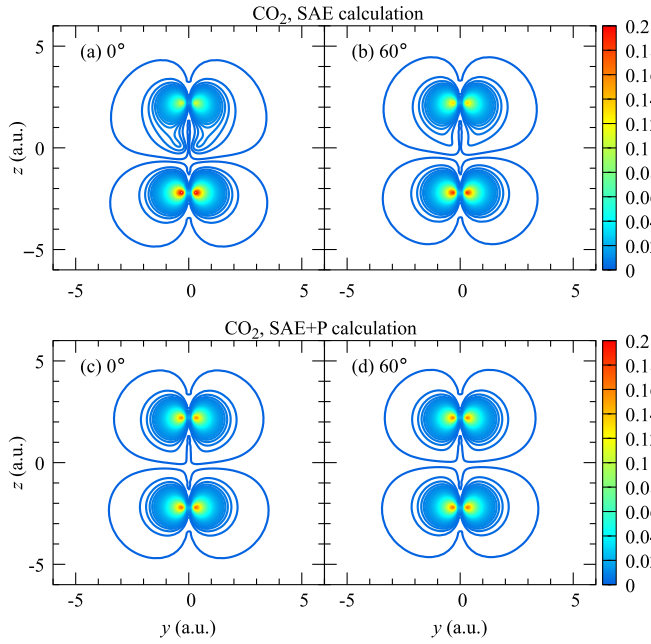


FIG. 4. Laser-deformed orbitals π_g of the CO_2 molecule subjected to the laser with above parameters for $\theta = 0^\circ$ (left panels) and $\theta = 60^\circ$ (right panels) when $|\mathbf{E}| = E_{\text{max}}$. The orbitals are calculated within SAE (top panels) and SAE + P (bottom panels) for $\phi_{\text{CEP}} = \pi$. The same result is obtained for $\phi_{\text{CEP}} = 3\pi/2$.

negligible. This point completes the argument in Ref. [71]. Moreover, as the distortion caused by the laser field is weaker when the molecule aligns at a higher angle from the laser field [compare Figs. 4(b) and 4(d)], the DCEP is less important. In fact, for our laser intensity of $2 \times 10^{14} \text{ W/cm}^2$, core polarization does not matter for $\theta > 60^\circ$.

In order to justify the reliability of our HHG spectra, we compare our results with some experimental data [15,21], focusing on the minimum position. To estimate the positions of minima, we use the smoothed spectra by averaging of three adjacent peaks and only consider the odd orders as measurable. The comparisons show the difference in the position between our simulation and these experiments is in the range of two harmonic orders. With $\theta \approx 30^\circ$, the minimum in Ref. [21] appears at the 23rd order; meanwhile, in our calculation, it locates at the 21st (SAE) and 25th (SAE + P) for $\phi_{\text{CEP}} = \pi$ and 23rd (SAE) and 25th (SAE + P) for $\phi_{\text{CEP}} = 3\pi/2$. Using the same laser parameters in Ref. [15] with the duration of 32 fs, and for the average value of $\langle \cos^2 \theta \rangle = 0.6-0.65$, i.e., $\theta \approx 38^\circ$, our HHG spectra exhibit the minima at about 44–47 eV in agreement with the strong minimum at $42 \pm 2 \text{ eV}$. It is noted that this difference may originate from the imperfect alignment in these experiments. Before using these minima to retrieve the structural information, we are going to discuss the relation between dipole forms and interference formulas in the next subsection.

B. Interference condition of CO_2 molecules

The interference effect in HHG can be explained by the two-center interference via the recombination matrix element

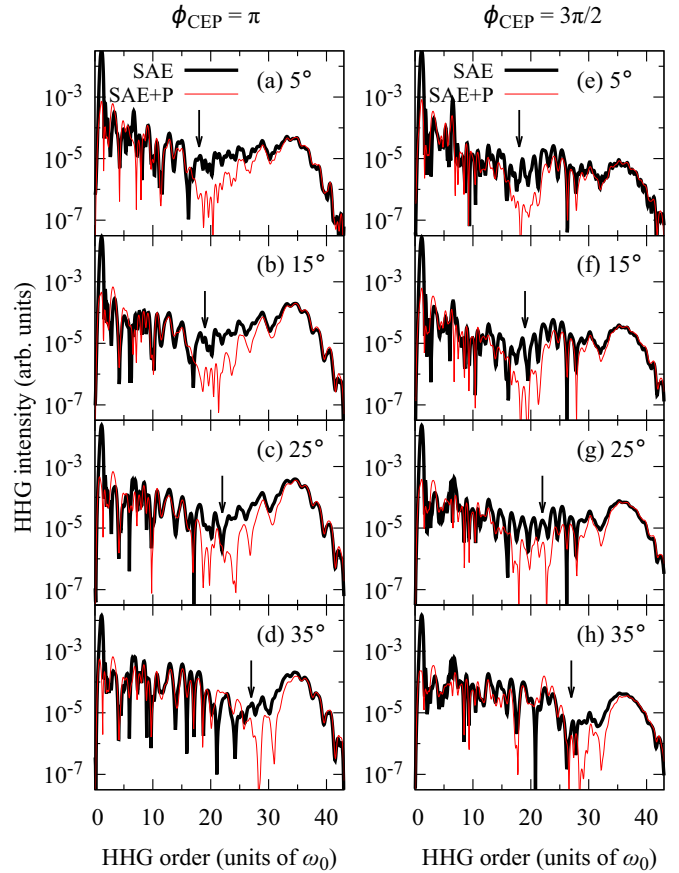


FIG. 5. Same as Fig. 3 but for $\theta = 5^\circ-35^\circ$. When the alignment angle increases, the minimum position also moves to higher orders. Arrows indicate the minimum locations predicted by the two-center interference model, Eq. (15).

[8,9]. Assume that the molecular orbital is a linear combination of atomic orbitals (LCAO) centered at each nucleus Φ_0

$$\Psi_0^\pm(\mathbf{r}) \propto \Phi_0(\mathbf{r} - \mathbf{R}/2) \pm \Phi_0(\mathbf{r} + \mathbf{R}/2), \quad (12)$$

where \mathbf{R} is the internuclear separation vector; then the matrix element is

$$\mathbf{d}(\mathbf{k}) = \langle e^{i\mathbf{k}\cdot\mathbf{r}} | \hat{O} | \Psi_0(\mathbf{r}) \rangle, \quad (13)$$

in which \hat{O} is the dipole operator in length, velocity, or acceleration forms, i.e., $\hat{O} = \mathbf{r}$, $\hat{O} = -i\nabla$, or $\hat{O} = \nabla V$, where V is the Coulomb potential.

If using the velocity or acceleration form, the conditions for destructive interference are [24,25,72,73]

$$R \cos \theta = (n - 1/2)\lambda \quad \text{for } \Psi_0^+, \quad (14)$$

$$R \cos \theta = n\lambda \quad \text{for } \Psi_0^-. \quad (15)$$

If using the length form, these conditions are interchanged [72,74]. Moreover, in the work of [74], we figured out the minima in perpendicular HHG spectra as well as the zero points of matrix element perpendicular to the molecular axis, named $d_y(k, \theta)$, obey Eq. (15). In Eqs. (14) and (15), $n = 1, 2, 3, \dots$ and λ is the de Broglie wavelength of a returning

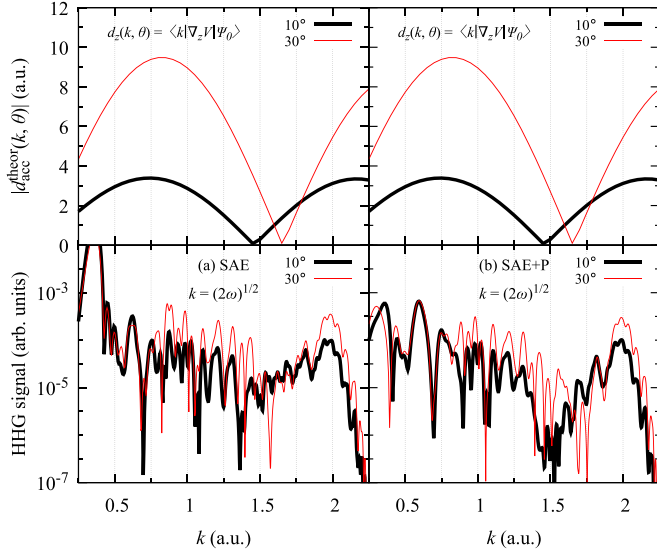


FIG. 6. Modulus of transition dipoles in the acceleration form with Ψ_0 obtained from TISE (top panels) and harmonic spectra from the CO_2 molecule as a function of wave number $k = \sqrt{2\omega}$. The calculations of HHG are carried out within SAE (a) and SAE + P (b) and illustrated for $\phi_{\text{CEP}} = \pi$ at $\theta = 10^\circ$ (thick black lines) and $\theta = 30^\circ$ (thin red lines).

electron. It connects to the harmonic order ω via the dispersion relation

$$k = \sqrt{2(\omega - \delta I_p)}, \quad (16)$$

where k is the wave number and $\delta = 0$ or $\delta = 1$ corresponds to different pictures when the electron recombines to the parent molecule ion [23,75–77]. In this paper, we use $\delta = 0$ as in Refs. [9,12] because it matches the minima of transition dipoles with those of our HHG spectra, Fig. 6. Actually, when one uses the length form for the dipole operator, the conditions for the interference are not as simple as Eqs. (14) and (15) [78]. However, if the CO_2 HOMO is constructed from the simple basis set in which only oxygen orbitals with the same symmetry are used, such as 3-21G of GAUSSIAN [54] or GAMESS [79], the minima of recombination matrix elements are in good agreement with Eq. (15) [80]. Once increasing the number of basis set such as 6-31+G(d,p), aug-cc-pVQZ or using the wave functions from the TISE, both the minima and the zero points of $d_y(k, \theta)$ will have discrepancy with Eq. (15) at some alignment angles about 30° – 45° [74] because of the contribution of carbon orbitals and all oxygen orbitals [24]. It should be noted that to make the minimum positions of HHG calculated from strong-field approximation consistent with that from solving the TDSE, one needs to consider the proper form of gauge in calculations [57,81,82] or add the Coulomb correction [78].

Now we discuss the relation between HHG spectra from the TDSE + SAE method and the form of the dipole operator. As shown in Fig. 6 for the laser with $\phi_{\text{CEP}} = \pi$, one can see the good agreement between the positions of minima in the HHG spectra from the TDSE + SAE method and those of the transition dipoles in the acceleration form. The correlation is the same for the laser with $\phi_{\text{CEP}} = 3\pi/2$ (not shown here).

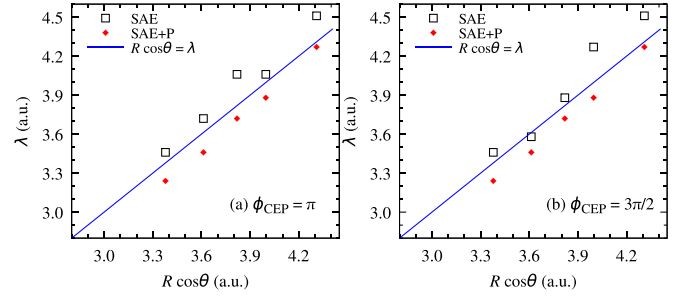


FIG. 7. Projection of the internuclear separation on the laser field direction and electron wavelength corresponding to the minima in the HHG spectra, $\lambda = 2\pi/\sqrt{2\omega_{\text{min}}}$, within SAE (black open squares), SAE + P (red diamonds), and the Bragg line $R \cos \theta = \lambda$ (blue lines). The results are implemented for the laser with (a) $\phi_{\text{CEP}} = \pi$ and (b) $\phi_{\text{CEP}} = 3\pi/2$.

This indicates that the interference formula Eq. (15) can be used for retrieving the internuclear distance.

C. Structural information from the interference minima

In this section, we illustrate the possibility of retrieving the structural information, the internuclear separation of CO_2 , using the two-center interference minima in the HHG spectra. With the laser parameters as mentioned, when the alignment angles are greater than about 43° , the interference minima do not exist in the plateau region of the spectra. Moreover, for some alignment angles, such as $\theta = 0^\circ$ for the two CEPs [Figs. 3(a) and 3(e)], $\theta = 25^\circ$ for $\phi_{\text{CEP}} = 3\pi/2$ [Fig. 5(g)], it is difficult to pinpoint the shallow minima in SAE without DCEP simulations. Based on the smoothed HHG spectra, our calculation results reveal that the interference effect occurs around the orders 17 ($\phi_{\text{CEP}} = \pi$) and 19 ($\phi_{\text{CEP}} = 3\pi/2$) in a large range of θ from 0° to about 20° . To improve the results, one can examine the alignment dependence of selected orders [10] and use the condition of phase jump [8,9,28,77] to determine the critical angle at where the interference effect occurs. However, because of the small change of $\cos \theta$ in the range of $[0^\circ$ – $20^\circ]$, the exact determination of the critical angle in this range has little improvement on the extracted result. Hence we average the value of $\cos \theta$ for the orders of 17 and 19. The results for both CEPs, Fig. 7(a) for π and Fig. 7(b) for $3\pi/2$, demonstrate that the minima obey the interference condition Eq. (15). We emphasize that the minima locations with DCEP included are unchanged with the two choices of CEP. This is probably because the DCEP brings the system closer to an ideal two-symmetric-points emitter whose interference pattern does not depend on laser parameters.

Now we extract the internuclear distance O–O of CO_2 based on the simulation results shown in Fig. 7 with the dispersion relation $k = \sqrt{2\omega}$. The results of the extracted bond length are presented in the tables.

Tables I and II show that the retrieval of the internuclear separation O–O from the interference minima has high accuracy with a small standard deviation and an error less than 4%. Moreover, the result is more stable against laser parameters (in this case CEP) and more accurate when considering the effect

TABLE I. Internuclear separation O–O of CO₂ obtained from the interference minima in the HHG spectra calculated within SAE and SAE + P for the laser with $\phi_{\text{CEP}} = \pi$.

θ (deg)	$\overline{\cos\theta}$	SAE			SAE + P		
		ω_{min}	R^* (a.u.)	Error (%)	ω_{min}	R^* (a.u.)	Error (%)
0							
5							
10	0.978	17	4.62	4.77	19	4.37	0.91
15							
20							
25	0.906	21	4.48	1.59	23	4.28	2.95
30	0.866	21	4.69	6.35	25	4.30	2.50
35	0.819	25	4.54	2.95	29	4.22	4.31
40	0.766	29	4.51	2.27	33	4.23	4.09
	Average		4.57	3.59		4.28	2.96
	Deviation (a.u.)		0.07			0.05	

of DCEP. With the fixed nuclei at the equilibrium distance, we also find out that the minima positions are unchanged with respect to the two CEPs for $\theta = 0^\circ$; see Figs. 3(a) and 3(e). This agrees with the result of Ref. [63] in which the authors investigated the influence of CEP on the minima of H₂⁺ when the molecule is parallel to the laser polarization. For higher θ , the same behavior is only obtained when the calculation includes the DCEP (refer to Fig. 5 or Tables I and II).

This retrieval's accuracy is comparable with that of another procedure using the laser-induced electron diffraction spectra [18]. Note that, despite the two methods being based on the assumption of perfect alignment, the internuclear separation is extracted from the harmonic spectrum with any given alignment angles, while this information can only be retrieved from the laser-induced electron diffraction if the molecule is aligned perpendicular to the laser polarization, i.e., $\theta = 90^\circ$. However, in reality, to fit well to experimental data, our model needs to account for the misalignment and the rovibrational dynamics of the molecule, first considered separately as in Ref. [18].

IV. CONCLUSION

In this work, we study and analyze the effect of dynamic core-electron polarization on the high-order harmonic generation for a nonpolar molecule CO₂ by numerically solving the time-dependent Schrödinger equation within the single active electron approximation. Besides, we also discuss the molecular structure in the interference effect, particularly the form of the dipole operator and the role of DCEP in retrieving the structural information.

Despite a small impact on the total ionization and ionization rate, the DCEP still affects the HHG spectra: the structural minima with the inclusion of DCEP appear deeper than those without the DCEP. Furthermore, the minima positions with DCEP included shift to higher energy. This effect is because the DCEP offsets the distortion of the orbital by the laser field. As a consequence, the extracted structural information is more accurate when considering the DCEP. The results indicate that, for a nonpolar molecule such as CO₂, the dynamic core polarization also plays an important role in the HHG process, especially the structural minima.

 TABLE II. Same as Table I but for $\phi_{\text{CEP}} = 3\pi/2$.

θ (deg)	$\overline{\cos\theta}$	SAE			SAE + P		
		ω_{min}	R^* (a.u.)	Error (%)	ω_{min}	R^* (a.u.)	Error (%)
0							
5							
10	0.978	17	4.62	4.77	19	4.32	0.91
15							
20							
25	0.906	19	4.71	6.81	23	4.28	2.95
30	0.866	23	4.48	1.59	25	4.30	2.50
35	0.819	27	4.37	0.91	29	4.22	4.31
40	0.766	29	4.51	2.27	33	4.23	4.09
	Average		4.54	3.27		4.28	2.96
	Deviation (a.u.)		0.10			0.05	

ACKNOWLEDGMENTS

We are funded by the Vietnam National Foundation for Science and Technology Development (NAFOSTED) under

Grant No. 103.01-2017.371. This work was carried out by the high performance computing cluster at Ho Chi Minh City University of Education, Vietnam.

-
- [1] A. McPherson, G. Gibson, H. Jara, U. Johann, T. S. Luk, I. A. McIntyre, K. Boyer, and C. K. Rhodes, *J. Opt. Soc. Am. B* **4**, 595 (1987).
- [2] M. Ferray, A. L'Huillier, X. F. Li, L. A. Lompre, G. Mainfray, and C. Manus, *J. Phys. B: At., Mol., Opt. Phys.* **21**, L31 (1988).
- [3] J. Itatani, J. Levesque, D. Zeidler, H. Niikura, H. Pepin, J. C. Kieffer, P. B. Corkum, and D. M. Villeneuve, *Nature (London)* **432**, 867 (2004).
- [4] S. Baker, J. S. Robinson, C. A. Haworth, H. Teng, R. A. Smith, C. C. Chirilă, M. Lein, J. W. G. Tisch, and J. P. Marangos, *Science* **312**, 424 (2006).
- [5] M. Uiberacker, T. Uphues, M. Schultze, A. J. Verhoef, V. Yakovlev, M. F. Kling, J. Rauschenberger, N. M. Kabachnik, H. Schröder, M. Lezius, K. L. Kompa, H.-G. Muller, M. J. J. Vrakking, S. Hendel, U. Kleineberg, U. Heinzmann, M. Drescher, and F. Krausz, *Nature (London)* **446**, 627 (2007).
- [6] D. Shafir, H. Soifer, B. D. Bruner, M. Dagan, Y. Mairesse, S. Patchkovskii, M. Y. Ivanov, O. Smirnova, and N. Dudovich, *Nature (London)* **485**, 343 (2012).
- [7] M. Mofared, E. Irani, and R. Sadighi-Bonabi, *Phys. Chem. Chem. Phys.* **21**, 9302 (2019).
- [8] M. Lein, N. Hay, R. Velotta, J. P. Marangos, and P. L. Knight, *Phys. Rev. Lett.* **88**, 183903 (2002).
- [9] M. Lein, N. Hay, R. Velotta, J. P. Marangos, and P. L. Knight, *Phys. Rev. A* **66**, 023805 (2002).
- [10] M. Lein, P. P. Corso, J. P. Marangos, and P. L. Knight, *Phys. Rev. A* **67**, 023819 (2003).
- [11] G. Lagmago Kamta and A. D. Bandrauk, *Phys. Rev. A* **70**, 011404(R) (2004).
- [12] G. L. Kamta and A. D. Bandrauk, *Phys. Rev. A* **71**, 053407 (2005).
- [13] A.-T. Le, X.-M. Tong, and C. D. Lin, *Phys. Rev. A* **73**, 041402(R) (2006).
- [14] S. Baker, J. S. Robinson, M. Lein, C. C. Chirilă, R. Torres, H. C. Bandulet, D. Comtois, J. C. Kieffer, D. M. Villeneuve, J. W. G. Tisch, and J. P. Marangos, *Phys. Rev. Lett.* **101**, 053901 (2008).
- [15] H. J. Wörner, J. B. Bertrand, P. Hockett, P. B. Corkum, and D. M. Villeneuve, *Phys. Rev. Lett.* **104**, 233904 (2010).
- [16] M. Labeye, F. Risoud, C. Lévêque, J. Caillat, A. Maquet, T. Shaaran, P. Salières, and R. Taïeb, *Phys. Rev. A* **99**, 013412 (2019).
- [17] T. Zuo, A. Bandrauk, and P. Corkum, *Chem. Phys. Lett.* **259**, 313 (1996).
- [18] M. Peters, T. T. Nguyen-Dang, E. Charron, A. Keller, and O. Atabek, *Phys. Rev. A* **85**, 053417 (2012).
- [19] K.-J. Yuan, H. Lu, and A. D. Bandrauk, *ChemPhysChem* **14**, 1496 (2013).
- [20] C. Vozzi, F. Calegari, E. Benedetti, J.-P. Caumes, G. Sansone, S. Stagira, M. Nisoli, R. Torres, E. Heesel, N. Kajumba, J. P. Marangos, C. Altucci, and R. Velotta, *Phys. Rev. Lett.* **95**, 153902 (2005).
- [21] T. Kanai, S. Minemoto, and H. Sakai, *Nature (London)* **435**, 470 (2005).
- [22] T. Kanai, E. J. Takahashi, Y. Nabekawa, and K. Midorikawa, *Phys. Rev. A* **77**, 041402(R) (2008).
- [23] X. Zhou, R. Lock, W. Li, N. Wagner, M. M. Murnane, and H. C. Kapteyn, *Phys. Rev. Lett.* **100**, 073902 (2008).
- [24] W. Boutu, S. Haessler, H. Merdji, P. Breger, G. Waters, M. Stankiewicz, L. J. Frasinski, R. Taïeb, J. Caillat, A. Maquet, P. Monchicourt, B. Carre, and P. Salieres, *Nat. Phys.* **4**, 545 (2008).
- [25] R. M. Lock, X. Zhou, W. Li, M. M. Murnane, and H. C. Kapteyn, *Chem. Phys.* **366**, 22 (2009).
- [26] R. Torres, T. Siegel, L. Brugnera, I. Procino, J. G. Underwood, C. Altucci, R. Velotta, E. Springate, C. Froud, I. C. E. Turcu, M. Y. Ivanov, O. Smirnova, and J. P. Marangos, *Opt. Express* **18**, 3174 (2010).
- [27] C. Vozzi, M. Negro, F. Calegari, G. Sansone, M. Nisoli, S. De Silvestri, and S. Stagira, *Nat. Phys.* **7**, 822 (2011).
- [28] T. T. Gorman, T. D. Scarborough, P. M. Abanador, F. Mauger, D. Kiesewetter, P. Sándor, S. Khatir, K. Lopata, K. J. Schafer, P. Agostini, M. B. Gaarde, and L. F. DiMauro, *J. Chem. Phys.* **150**, 184308 (2019).
- [29] A. Etches and L. B. Madsen, *J. Phys. B: At., Mol., Opt. Phys.* **43**, 155602 (2010).
- [30] A. Etches, M. B. Gaarde, and L. B. Madsen, *Phys. Rev. A* **84**, 023418 (2011).
- [31] X. Zhu, Q. Zhang, W. Hong, P. Lan, and P. Lu, *Opt. Express* **19**, 436 (2011).
- [32] A. Rupenyan, P. M. Kraus, J. Schneider, and H. J. Wörner, *Phys. Rev. A* **87**, 031401(R) (2013).
- [33] F. Mauger, P. M. Abanador, T. D. Scarborough, T. T. Gorman, P. Agostini, L. F. DiMauro, K. Lopata, K. J. Schafer, and M. B. Gaarde, *Struct. Dyn.* **6**, 044101 (2019).
- [34] B. Zimmermann, M. Lein, and J. M. Rost, *Phys. Rev. A* **71**, 033401 (2005).
- [35] M. Gühr, B. K. McFarland, J. P. Farrell, and P. H. Bucksbaum, *J. Phys. B: At., Mol., Opt. Phys.* **40**, 3745 (2007).
- [36] Y. Mairesse, J. Levesque, N. Dudovich, P. Corkum, and D. Villeneuve, *J. Mod. Opt.* **55**, 2591 (2008).
- [37] B. K. McFarland, J. P. Farrell, P. H. Bucksbaum, and M. Gühr, *Phys. Rev. A* **80**, 033412 (2009).
- [38] J. P. Farrell, B. K. McFarland, M. Gühr, and P. H. Bucksbaum, *Chem. Phys.* **366**, 15 (2009).
- [39] T. K. Kjeldsen and L. B. Madsen, *Phys. Rev. A* **73**, 047401 (2006).
- [40] M. D. Śpiewanowski, A. Etches, and L. B. Madsen, *Phys. Rev. A* **87**, 043424 (2013).
- [41] B. K. McFarland, J. P. Farrell, P. H. Bucksbaum, and M. Gühr, *Science* **322**, 1232 (2008).
- [42] O. Smirnova, Y. Mairesse, S. Patchkovskii, N. Dudovich, D. Villeneuve, P. Corkum, and M. Y. Ivanov, *Nature (London)* **460**, 972 (2009).

- [43] E. P. Fowe and A. D. Bandrauk, *Phys. Rev. A* **81**, 023411 (2010).
- [44] M. Ruberti, P. Decleva, and V. Averbukh, *Phys. Chem. Chem. Phys.* **20**, 8311 (2018).
- [45] Z. Zhao and T. Brabec, *J. Mod. Opt.* **54**, 981 (2007).
- [46] G. Jordan and A. Scrinzi, *New J. Phys.* **10**, 025035 (2008).
- [47] B. Zhang, J. Yuan, and Z. Zhao, *Phys. Rev. Lett.* **111**, 163001 (2013).
- [48] Z. Zhao and J. Yuan, *Phys. Rev. A* **89**, 023404 (2014).
- [49] B. Zhang, J. Yuan, and Z. Zhao, *Phys. Rev. A* **90**, 035402 (2014).
- [50] V.-H. Hoang, S.-F. Zhao, V.-H. Le, and A.-T. Le, *Phys. Rev. A* **95**, 023407 (2017).
- [51] C.-T. Le, V.-H. Hoang, L.-P. Tran, and V.-H. Le, *Phys. Rev. A* **97**, 043405 (2018).
- [52] A. Rupenyany, P. M. Kraus, J. Schneider, and H. J. Wörner, *Phys. Rev. A* **87**, 033409 (2013).
- [53] M. Abu-samha and L. B. Madsen, *Phys. Rev. A* **81**, 033416 (2010).
- [54] M. J. Frisch, G. W. Trucks, H. B. Schlegel *et al.*, *Gaussian 03, Revision C.02*, Gaussian, Inc., Wallingford, CT, 2004.
- [55] R. van Leeuwen and E. J. Baerends, *Phys. Rev. A* **49**, 2421 (1994).
- [56] H. Bachau, E. Cormier, P. Decleva, J. E. Hansen, and F. Martín, *Rep. Prog. Phys.* **64**, 1815 (2001).
- [57] C. C. Chirilă and M. Lein, *J. Mod. Opt.* **54**, 1039 (2007).
- [58] J. C. Baggesen and L. B. Madsen, *J. Phys. B* **44**, 115601 (2011).
- [59] A. D. Bandrauk, S. Chelkowski, D. J. Diestler, J. Manz, and K.-J. Yuan, *Phys. Rev. A* **79**, 023403 (2009).
- [60] K. Burnett, V. C. Reed, J. Cooper, and P. L. Knight, *Phys. Rev. A* **45**, 3347 (1992).
- [61] G. L. Kamta and A. D. Bandrauk, *Phys. Rev. Lett.* **94**, 203003 (2005).
- [62] G. L. Kamta, A. D. Bandrauk, and P. B. Corkum, *J. Phys. B: At., Mol., Opt. Phys.* **38**, L339 (2005).
- [63] P. Hu, Y. Niu, Y. Xiang, S. Gong, and C. Liu, *Opt. Express* **23**, 23834 (2015).
- [64] B. Wang, L. He, H. Yuan, Q. Zhang, P. Lan, and P. Lu, *Opt. Express* **26**, 33440 (2018).
- [65] D. A. Telnov, K. Nasiri Avanaki, and S.-I. Chu, *Phys. Rev. A* **90**, 043404 (2014).
- [66] T. K. Kjeldsen and L. B. Madsen, *J. Phys. B: At., Mol., Opt. Phys.* **37**, 2033 (2004).
- [67] M. Yuan, P. Xin, T. Chu, and H. Liu, *Opt. Express* **25**, 23493 (2017).
- [68] I. A. Ivanov, C. Hofmann, L. Ortmann, A. S. Landsman, C. H. Nam, and K. T. Kim, *Commun. Phys.* **1**, 81 (2018).
- [69] M. Lewenstein, P. Balcou, M. Y. Ivanov, A. L'Huillier, and P. B. Corkum, *Phys. Rev. A* **49**, 2117 (1994).
- [70] M. Qin, X. Zhu, Y. Li, Q. Zhang, P. Lan, and P. Lu, *Phys. Rev. A* **89**, 013410 (2014).
- [71] M. D. Śpiewanowski and L. B. Madsen, *Phys. Rev. A* **89**, 043407 (2014).
- [72] G. N. Gibson and J. Biegert, *Phys. Rev. A* **78**, 033423 (2008).
- [73] S. Haessler, W. Boutu, H. Merdji, P. Breger, R. Taïeb, J. Caillat, A. Maquet, P. Monchicourt, B. Carré, and P. Salières, *Measuring the Complex Recombination Dipole of Aligned CO₂ Molecules in High-order Harmonic Generation*, UVX 2008 (EDP Sciences, London, 2009), p. 65.
- [74] C.-T. Le, V.-H. Hoang, N.-T. Nguyen, and V.-H. Le, *Mater. Trans.* **56**, 1441 (2015).
- [75] J. Levesque, D. Zeidler, J. P. Marangos, P. B. Corkum, and D. M. Villeneuve, *Phys. Rev. Lett.* **98**, 183903 (2007).
- [76] I. Gonoskov and M. Ryabikin, *J. Mod. Opt.* **55**, 2685 (2008).
- [77] E. V. van der Zwan and M. Lein, *Phys. Rev. A* **82**, 033405 (2010).
- [78] M. F. Ciappina, C. C. Chirilă, and M. Lein, *Phys. Rev. A* **75**, 043405 (2007).
- [79] M. W. Schmidt, K. K. Baldrige, J. A. Boatz, S. T. Elbert, M. S. Gordon, J. H. Jensen, S. Koseki, N. Matsunaga, K. A. Nguyen, S. Su, T. L. Windus, M. Dupuis, and J. A. Montgomery, *J. Comput. Chem.* **14**, 1347 (1993).
- [80] R. Torres and J. P. Marangos, *J. Mod. Opt.* **54**, 1883 (2007).
- [81] C. C. Chirilă and M. Lein, *Phys. Rev. A* **73**, 023410 (2006).
- [82] C. Figueira de Morisson Faria, *Phys. Rev. A* **76**, 043407 (2007).